ARTICLE
Journal of Cellular Biochemistry 112:1176–1191 (2011)

Journal of Cellular Biochemistry

Destabilization of CARP mRNAs by Aloe-Emodin Contributes to Caspase-8-Mediated p53-Independent Apoptosis of Human Carcinoma Cells

Meng-Liang Lin,[1] Yao-Cheng Lu,[2] Hong-Lin Su,[2] Hsin-Ting Lin,[3] Chuan-Chun Lee,[1] Shang-En Kang,[3] Tan-Chen Lai,[3] Jing-Gung Chung,[4] and Shih-Shun Chen[3]*

[1]*Department of Medical Laboratory Science and Biotechnology, China Medical University, Taichung, Taiwan*

[2]*Department of Life Sciences, National Chung Hsing University, Taichung, Taiwan*

[3]*Department of Medical Laboratory Science and Biotechnology, Central Taiwan University of Science and Technology, Taichung, Taiwan*

[4]*Department of Biological Science and Technology, China Medical University, Taichung, Taiwan*

ABSTRACT

Using short hairpin RNA against p53, transient ectopic expression of wild-type p53 or mutant p53 (R248W or R175H), and a p53- and p21-dependent luciferase reporter assay, we demonstrated that growth arrest and apoptosis of FaDu (human pharyngeal squamous cell carcinoma), Hep3B (hepatoma), and MG-63 (osteosarcoma) cells induced by aloe-emodin (AE) are p53-independent. Co-immunoprecipitation and small interfering RNA (siRNA) studies demonstrated that AE caused S-phase cell cycle arrest by inducing the formation of cyclin A–Cdk2–p21 complexes through extracellular signal-regulated kinase (ERK) activation. Ectopic expression of Bcl-X_L and siRNA-mediated Bax attenuation significantly inhibited apoptosis induced by AE. Cyclosporin A or the caspase-8 inhibitor Z-IETD-FMK blocked AE-induced loss of mitochondrial membrane potential and prevented increases in reactive oxygen species and Ca^{++}. Z-IETD-FMK inhibited AE-induced apoptosis, Bax expression, Bid cleavage, translocation of tBid to mitochondria, ERK phosphorylation, caspase-9 activation, and the release of cytochrome *c*, apoptosis-inducing factor (AIF), and endonuclease G from mitochondria. The stability of the mRNAs encoding caspase-8 and -10-associated RING proteins (CARPs) 1 and 2 was affected by AE, whereas CARP1 or 2 overexpression inhibited caspase-8 activation and apoptosis induced by AE. Collectively, our data indicate AE induces caspase-8-mediated activation of mitochondrial death pathways by decreasing the stability of CARP mRNAs in a p53-independent manner. J. Cell. Biochem. 112: 1176–1191, 2011.

KEY WORDS: ALOE-EMODIN; CARP; CASPASE-8; CDK2; CHINESE HERB; E2F1; ERK; MITOCHONDRIAL DEATH PATHWAY; TBID; ENDO G; AIF; ROS

The transcriptional regulation and tumor suppressor functions of p53 are commonly lost in human cancers. More than ~50% of human cancers show mutations or deletion of the *P53* gene, which is associated with a poor response to various types of therapies [Nylander et al., 2000]. Identifying drugs that induce p53-independent apoptosis of cancer cells is therefore urgently needed.

Mitochondria are considered the main target for the apoptosis induction that occurs in response to a variety of stress stimuli, such as growth factor withdrawal, γ-irradiation, and chemotherapeutic drugs. The mitochondrial death pathway is initiated by the disruption of the outer mitochondrial membrane, and it involves the release of cytochrome *c*, second mitochondria-derived activator of caspase/direct inhibitor of apoptosis-binding protein with low pI (Smac/DIABLO), apoptosis-inducing factor (AIF), and endonuclease G (Endo G) from mitochondria into the cytosol [Tsujimoto, 2003]. Cytosolic cytochrome *c* can trigger the proteolytic processing of pro-caspase-9, initiating the formation of an apoptosome composed of Apaf-1, dATP, caspase-9, and cytochrome *c*. Apoptosome formation leads to the activation of executioner caspase-3, -6, and -7 [Budihardjo et al., 1999]. Nuclear translocation of AIF and Endo G

Grant sponsor: China Medical University, Taiwan; Grant number: CMU98-C-06; Grant sponsor: Taichung Veterans General Hospital and Central Taiwan University of Science and Technology, Taiwan; Grant number: TCVGH-CTUST987715.

*Correspondence to: Prof. Shih-Shun Chen, Department of Medical Laboratory Science and Biotechnology, Central Taiwan University of Science and Technology, No. 666, Buzih Road, Beitun District, Taichung 40601, Taiwan.
E-mail: sschen1@ctust.edu.tw

Received 7 August 2010; Accepted 14 January 2011 • DOI 10.1002/jcb.23031 • © 2011 Wiley-Liss, Inc.
Published online 1 February 2011 in Wiley Online Library (wileyonlinelibrary.com).

occurs and can induce DNA fragmentation and apoptotic cell death in a caspase-independent manner [Penninger and Kroemer, 2003]. The release of Endo G and AIF from the mitochondria in response to pro-apoptotic stimuli is, however, caspase-dependent [Arnoult et al., 2003]. Members of the Bcl-2 family, such as Bcl-2/Bcl-X_L and Bax/Bak, can both negatively and positively regulate mitochondrial events that occur during apoptotic cell death by suppressing cytochrome *c* release [Brunelle and Letai, 2009]. Several studies have shown that chemotherapeutic agent-induced apoptosis involves the cleavage of cytosolic Bid to truncated Bid (tBid) by caspase-8 [Anto et al., 2002; Kim et al., 2009]. tBid induces pro-apoptotic protein Bax oligomerization and the generation of the mitochondrial permeability transition pore, which leads to the loss of mitochondrial membrane potential ($\Delta\psi_m$) and to cytochrome *c* release [Ott et al., 2009]. Caspase-8 and -10-associated RING proteins (CARPs), new members of the inhibitor of apoptotic protein family, have been shown to interact specifically with caspase-8 and regulate its processing via ubiquitin-mediated proteolysis [McDonald and El-Deiry, 2004]. Transient small interfering RNA (siRNA)-mediated attenuation of CARP expression can inhibit tumor cell growth. In addition, overexpression of CARPs in cancer cells blocks death ligand-induced apoptosis [McDonald and El-Deiry, 2004].

Among the mitogen-activated protein kinase (MAPK) family members, extracellular signal-regulated kinase (ERK)-mediated signaling is typically associated with mitogen- and growth factor-induced cell differentiation, cell proliferation, and survival [Hill and Treisman, 1995], whereas the p38 MAPK and c-Jun N-terminal kinase (JNK) pathways are involved in cell growth inhibition and apoptosis [Xia et al., 1995]. However, increasing evidence suggests that the complicated roles of these MAPK pathways exist to transmit distinct cellular effects in different cell types [Dhillon et al., 2007]. ERK activation is involved in the p53-independent induction of S-phase arrest and p21 expression in DLD-1 (human colon cancer) and HL-60 (promyelocytic leukemia) cell lines [Zhu et al., 2004; Song et al., 2008]. In contrast, p38 MAPK and JNK activities are associated with anti-apoptosis [Chao et al., 2004] and cancer invasion [Pan et al., 2009].

Aloe-emodin (AE) (1,8-dihydroxy-3-(hydroxymethyl) anthraquinone) is isolated from the rhizomes of *Rheum palmatum*. AE-induced G_1-phase cell cycle arrest in human hepatoma HepG2 cell lines is associated with p53 and p21 up-regulation [Kuo et al., 2002]. Furthermore, JNK activation is involved in AE-induced apoptotic cell death of the human hepatoma HepG2 cell line [Lu et al., 2007]. The inhibition of ERK activity causes the induction of cell differentiation, but not of apoptosis, in AE-treated rat C6 glioma cells [Mijatovic et al., 2005]. Herein, we demonstrate that the induction of p53-independent apoptosis by AE occurs through the caspase-8-mediated activation of the mitochondrial death pathway by decreasing the stability of CARP mRNAs and that the increases in p21 and E2F1 expression and S-phase arrest are mediated by ERK activation.

MATERIALS AND METHODS

CHEMICALS

AE, actinomycin D, cyclosporine A (CsA), dantrolene, NP-40, paraformaldehyde, PD98059, propidium iodide (PI), Tris–HCl, 4′-6-diamidino-2-phenylindole (DAPI), and Triton X-100 were obtained from Sigma-Aldrich (St. Louis, MO). AE was dissolved in and diluted with DMSO and then stored at −20°C as a 100 mM stock. Potassium phosphate was purchased from Merck (Darmstadt, Germany). Lipofectamine 2000 was obtained from Invitrogen (Carlsbad, CA). Dulbecco's modified Eagle's medium (DMEM), whereas minimum essential medium (MEM), fetal bovine serum (FBS), trypsin–EDTA, glutamine, and puromycin were obtained from Gibco BRL (Grand Island, NY). The caspase-3 activity assay kit was purchased from OncoImmunin (Gaithersburg, MD). Caspase-8 and -9 activity assay kits were obtained from Calbiochem (San Diego, CA). Inhibitors of pan-caspase (Z-VAD-FMK), caspase-3 (Ac-DEVD-CMK), caspase-4 (LEVD-CHO), caspase-8 (Z-IETD-FMK), and caspase-9 (Z-LEHD-FMK) were purchased from Calbiochem (San Diego) and were all dissolved in DMSO. pPuro-p53 shRNA, pPuro-GFP shRNA, pFLAG-CMV2-CARP1, and pFLAG-CMV2-CARP2 vectors were obtained from Addgene (Cambridge, MA). Bax siRNA, Bak siRNA, and Western Blotting Luminol Reagent were purchased from Santa Cruz Biotechnology (Santa Cruz, CA). Bax siRNA and Bak siRNA were dissolved in RNase-free water. The double-stranded siRNA sequences were as follows: Bax siRNA, 5′-GGUGCCGGAACUGAUCAGA-3′/3′-UCUGAUCAGUUCCGGCACC-5′ and 5′-AACAUGGAGCUGCAGAGGAUGA-3′/3′-UCAUCCUCUGCAGCUCCAUGUU-5′; Bak siRNA, 5′-CCGACGCUAUGACUCAGAGTT-3′/3′-CUCUGAGUCAUAGCGUCGGTT-5′; ERK siRNA, 5′-GCAAUGACCAUAUCUGCUA(dTdT)-3′/3′-(TdTd)CGUUACUGGUAU AGACGAU-5′. The primer sequences were as follows: CARP1, 5′-AACGCAGAGGATCGGAACC-3′ and 5′-TTCCACATCATC AAGGCTTGAC-3′; CARP2, 5′-AGCATGGTTCCACCTACCTCAC-3′ and 5′-CCTCTTGATCCTGAGACACATGG-3′ [McDonald and El-Deiry, 2004]; p53, 5′-TGCGTGTGGAGTATTTGGATG-3′ and 5′-TGACCCTTTTTGGACTTCAG-3′; β-actin, 5′-GCTTGACTCAGGATTTAAAAACTGGAACGG-3′ and 5′-TATTCAACTGGTCTCAAGTCAGTGTACAGG-3′.

ANTIBODIES

Antibodies against cyclin A, cyclin B, cyclin D, cyclin E, Cdk2, phospho (p)-Cdk2 (Thr14/Thr15), Bak, Bad, Bid, tBid, NOXA, MCL-1, Bik, BIM, PUMA, Endo G, AIF, p53, p21, E2F1, and proliferating cell nuclear antigen (PCNA) were purchased from Santa Cruz Biotechnology. Antibodies against ERK, p-ERK (Tyr202/204), Bcl-2, Bcl-X_L, Bax, and cytochrome *c* were obtained from BD Pharmingen (San Diego, CA). Antibodies against caspase-3, -8, and tBid were purchased from Calbiochem (San Diego). Anti-cytochrome *c* oxidase subunit II (Cox2) was obtained from Abcam (Cambridge, MA). Antibodies against γ-tubulin and FLAG-tag were purchased from Sigma-Aldrich. Peroxidase-conjugated anti-mouse IgG, -goat IgG, and -rabbit IgG secondary antibodies were purchased from Jackson ImmunoResearch Laboratory (West Grove, PA).

CELL CULTURE

The human pharyngeal squamous cell carcinoma line FaDu, the human lung cancer cell line H1299, the human hepatoma cell line Hep3B, the human osteosarcoma cell line MG-63, normal human embryonic lung fibroblasts (WI-38), normal human fetal skin fibroblasts (Detroit 551), normal embryonic lung fibroblasts (MRC-5), the normal mouse embryonic liver cell line BNL CL.2, and

human embryonic kidney 293 cells were obtained from the Food Industry Research and Development Institute (Hsinchu, Taiwan). FaDu, RPMI 2650, WI-38, Detroit 551, and MRC-5 cell lines were cultured in MEM supplemented with 5% FBS. The 293, H1299, Hep3B, and MG-63 cell lines were cultured routinely in DMEM supplemented with 5% FBS. All cell lines were grown in 10-cm tissue culture dishes at 37°C in a humidified incubator containing 5% CO_2.

ESTABLISHMENT OF CELL CLONES PERMANENTLY EXPRESSING P53 shRNA OR GFP shRNA

To establish cells stably expressing p53 shRNA or GFP shRNA, cells were transfected using Lipofectamine 2000 with pPuro-p53 shRNA or pPuro-GFP shRNA plasmid. The transfected cells were selected and cloned in the presence of 2 μg/ml puromycin. The efficiency of p53 knockdown was confirmed by Western blot analysis with anti-p53 antibody.

CELL VIABILITY ASSAY

Cells were seeded at 3×10^4 cells/well in 24-well tissue culture plates. Cells were grown overnight to ~60% confluence and treated with either DMSO (vehicle control) or AE for the indicated times. In the controls, DMSO was diluted in culture medium to the same final concentration (0.01%, v/v) as in the medium with AE. At the end of the incubation, treated cells were harvested and stained with PI solution (10 μg/ml in phosphate-buffered saline (PBS)). Samples were analyzed on a FACSCount flow cytometer (BD Biosciences, Franklin Lakes, NJ). Cell Quest software (BD Biosciences) was used to analyze the results. PI-negative populations were defined as viable cells. Cell morphology was observed using an inverted phase contrast and fluorescence microscope (IX71; Olympus, Inc., Melville, NY).

MTT ASSAY

The cells were seeded at a density of 3×10^4 cells per well into 24-well plates. After 16 h of incubation, cells were grown to ~60% confluence and treated with either vehicle or 60 μM AE at 37°C for the indicated times before being harvested. The treated cells were washed once with PBS and incubated with 0.5 mg/ml MTT for 5 h. The resulting formazan precipitate was dissolved in 150 μl of DMSO and the optical density (OD) of formazan was determined using an ELISA reader (Thermo Labsystems Multiskan Spectrum, Franklin, MA) at 570 nm.

RT-PCR

RNA was extracted using Trizol reagent (Invitrogen Life Technologies, Carlsbad, CA). First-strand cDNA was made using 1 μg of total RNA in the presence of Superscript II reverse transcriptase (Gibco BRL) and random hexamers. cDNA was PCR-amplified using Vent DNA polymerase (NEB BioLabs) and specific primers corresponding directly to a region in the *P53*, *CARP1*, or *CARP2* gene. Samples were taken from the PCR mixture after 25 or 35 cycles of amplification, separated on a 1.5% agarose gel, and stained with ethidium bromide.

MEASUREMENT OF DNA FRAGMENTATION

Histone-associated DNA fragments were determined using the Cell Death Detection enzyme-linked immunosorbent assay (ELISA) kit (Roche Applied Science, Mannheim, Germany). Briefly, vehicle- or AE-treated cells were incubated in hypertonic buffer for 30 min at room temperature. After centrifugation, the cell lysates were transferred into an anti-histone-coated microplate to bind histone-associated DNA fragments. Plates were washed after 1.5 h of incubation, and non-specific binding sites were saturated with blocking buffer. Plates were then incubated with peroxidase-conjugated anti-DNA for 1.5 h at room temperature. To determine the amount of retained peroxidase, 2,2′-azino-di-(3-ethylbenzthiazoline-6-sulfonate) was added as a substrate, and a spectrophotometer (Thermo Labsystems Multiskan Spectrum) was used to measure the absorbance at 405 nm.

p53 AND p21 PROMOTER ASSAY

p53-knockdown cells were seeded at a concentration of 5×10^4 cells per well in 12-well tissue culture plates and grown overnight to ~70% confluency. A luciferase reporter driven by three p53 binding sites or by the p21 promoter and a plasmid expressing wild-type (wt) p53, mutant p53 (R248W), or p53 (R175H) were transfected into cells using Lipofectamine 2000. The β-galactosidase expression vector pCH110 was included as an internal control. At 12 h post-transfection, cells were treated with vehicle or AE for 24 h. The cell lysates were harvested, and the protein expression and luciferase activity were determined using Western blot analysis and the Dual-Luciferase Reporter Assay kit (Promega, Madison, WI), respectively. The value of luciferase activity was normalized to transfection efficiency as monitored by β-galactosidase expression.

ASSAY FOR CASPASE-3 ACTIVITY

Caspase-3 activity was measured using the PhiPhiLux G1D2 kit (OncoImmunin, College Park, MD). Briefly, vehicle- or AE-treated cells were incubated with PhiPhiLux fluorogenic caspase substrate for 1 h at 37°C, washed three times with PBS, resuspended in 500 μl of ice-cold PBS, and analyzed on a FACSCount flow cytometer.

MEASUREMENT OF CELL CYCLE BY FLOW CYTOMETRY

Cells (1×10^5) were trypsinized, washed twice with PBS, and fixed in 80% ethanol. Fixed cells were washed with PBS, incubated with 100 μg/ml RNase for 30 min at 37°C, stained with PI (50 μg/ml), and analyzed on a FACSCount flow cytometer. The percentage of cells that had undergone apoptosis was assessed as the ratio of the area of fluorescence that was smaller than the G_0–G_1 peak to the total area of fluorescence.

CO-IMMUNOPRECIPITATION ASSAY

p53 shRNA-expressing stable cells (5×10^5) were treated with 60 μM of AE for the indicated periods. Cells were harvested and lysed in 0.6 ml of cell lysis buffer (50 mM Tris–HCl (pH 8.0), 150 mM NaCl, 1 mM Na_2EDTA, 100 mM Na_3VO_4, 0.5% (v/v) NP-40, 50 mM NaF, 25 mM leupeptin). Whole-cell extracts were incubated with anti-Cdk2, anti-cyclin A, or normal mouse IgG as a negative control at 4°C for 2 h. After incubation, protein A–agarose beads (Amersham Biosciences, Piscataway, NJ) were added, and the mixture was

incubated with gentle rocking at 4°C for 2 h. The immunocomplexes were then analyzed by 10% SDS–PAGE and immunoblotted with antibodies against cyclin A, Cdk2, p21, PCNA, and E2F1.

WESTERN BLOT ANALYSIS

Treated or transfected cells were lysed in lysis buffer (50 mM Tris–HCl (pH 8.0), 120 mM NaCl, 1 μg/ml aprotinin, 100 mM Na_3VO_4, 50 mM NaF, 0.5% NP-40). Protein concentration was determined by the Bradford method (Bio-Rad, Hercules, CA). Proteins were separated by electrophoresis on a 10% SDS–PAGE gel and then transferred to polyvinylidene difluoride membranes (Immobilon-P; Millipore, Bedford, MA). Membranes were blocked overnight with PBS containing 3% skim milk and then incubated with primary antibody against cyclin A, cyclin B, cyclin D, cyclin E, Cdk2, p-Cdk2 (Thr14/Thr15), E2F1, PCNA, p53, p21, ERK, p-ERK (Tyr202/204), Bcl-X_L, Bcl-2, Bax, Bak, Bid, tBid, caspase-3, caspase-8, caspase-9, cytochrome *c*, AIF, Endo G, or Cox2. Proteins were detected with horseradish peroxidase-conjugated goat anti-mouse, goat anti-rabbit, or donkey anti-goat antibodies and the Western Blotting Luminol Reagent. To confirm equal protein loading, γ-tubulin was measured.

PLASMID AND siRNA TRANSFECTION

Cells (at 70% confluency in a 12-well plate) were transfected with FLAG epitope-tagged Bcl-X_L or Bcl-2 expression plasmid or with Bax, Bak and ERK (pKD-MAPK1/Erk) siRNAs using Lipofectamine 2000. The expression of FLAG-Bcl-X_L, FLAG-Bcl-2, Bax, and Bak in transfected cells was assessed by Western blotting using antibodies specific against FLAG, Bax, or Bak.

DETECTION OF CYTOCHROME *C*, AIF, AND ENDO G

Treated cells were first lysed in isotonic mitochondrial buffer (210 mM mannitol, 70 mM sucrose, 1 mM EDTA, 10 mM HEPES (pH 7.5)) and homogenized with 30–40 strokes of a Dounce homogenizer (Dounce; Bellco Glass Co., Vineland, NJ). Nuclei and unbroken cells were removed by centrifugation at 500*g* for 5 min at 4°C in a microcentrifuge. Supernatants were then centrifuged at 10,000*g* for 30 min at 4°C, and the resulting supernatants were stored as the cytosolic fraction. Total proteins (20 μg) were separated by 12% SDS–PAGE and were transferred onto polyvinylidene difluoride membranes, which were then incubated with primary antibodies against cytochrome *c*, AIF, and Endo G. Proteins were detected with horseradish peroxidase-conjugated goat anti-mouse or goat anti-rabbit antibodies and the Western Blotting Luminol Reagent. γ-Tubulin and Cox2 were used as internal controls for sample loading.

MEASUREMENT OF MITOCHONDRIAL MEMBRANE POTENTIAL

Mitochondrial membrane potential ($\Delta\psi_m$) was determined by measuring the retention of the dye 3,3′-dihexyloxacarbocyanine ($DiOC_6$). Briefly, cells treated with vehicle, AE (60 μM), AE (60 μM) plus CsA (5 μM), AE (60 μM) plus dantrolene (25 μM), or AE (60 μM) plus Z-IETD-FMK (40 μM) were incubated with 40 nM $DiOC_6$ for 30 min at 37°C. Cells were then pelleted by centrifugation at 160*g*. Pellets were resuspended and washed twice with PBS. The $\Delta\psi_m$ was determined with a FACSCount flow cytometer.

DETECTION OF REACTIVE OXYGEN SPECIES

Overnight-cultured cells (1×10^5 cells) were treated with vehicle, AE (60 μM), AE (60 μM) plus CsA (5 μM), AE (60 μM) plus dantrolene (25 μM), or AE (60 μM) plus Z-IETD-FMK (40 μM) for 1, 3, 6, or 12 h to detect changes in reactive oxygen species (ROS). After treatment, cells were harvested and washed twice with PBS. Cells were then resuspended in 500 μl of 2,7-dichlorodihydrofluorescein diacetate (10 μM) and incubated for 30 min at 37°C. The level of ROS was determined using a FACSCount flow cytometer.

MEASUREMENT OF CYTOSOLIC Ca^{++}

Briefly, cells treated with vehicle, AE (60 μM), AE (60 μM) plus CsA (5 μM), AE (60 μM) plus Z-IETD-FMK (40 μM), or AE (60 μM) plus dantrolene (25 μM) were incubated with 3 μg/ml of Indo-1/AM (Calbiochem, La Jolla, CA) and incubated for 30 min at 37°C. After washing twice with assay buffer, cells were suspended in assay buffer (Calbiochem, La Jolla). The level of Ca^{++} was determined using a FACSCount flow cytometer.

STATISTICAL ANALYSIS OF DATA

Statistical calculations were performed using the unpaired Student's *t*-test and ANOVA. Statistical significance between vehicle control and experimental groups was set at $P < 0.05$.

RESULTS

AE INDUCES p53-INDEPENDENT APOPTOTIC CELL DEATH

The first study used the mutant p53 (R248L)-carrying human cell line FaDu and the p53-null-carrying human cancer cell lines H1299, Hep3B, and MG-63. PI staining and flow-cytometric analysis showed that AE significantly reduced FaDu, H1299, Hep3B, and MG-63 cell viability in a dose-dependent manner (Fig. 1A, panel I). Treatment for 36 h with 60 μM AE in FaDu, Hep3B, and MG-63 cells resulted in 49.74%, 46.82%, and 53.46% reductions in cell viability, respectively. The IC_{50} value of AE in these cells was 60 μM, which was then used in all subsequent experiments (panel II). In contrast, 60 μM AE was less toxic to human normal cell lines (WI-38, Detroit 551, MRC-5, and 293 cells) and normal mouse liver cells [Lin et al., 2010]. To rule out the possibility that mutated p53 (R248L) or endogenous p53 were still functional, we used cells stably expressing a shRNA to knock down p53 and examined the effect of AE on these cells. p53 mRNA and protein levels were reduced in cells expressing the shRNA, demonstrating efficient and stable knock-down (Fig. 1B, panel I). No change in caspase-3 activity or apoptosis was observed in p53 shRNA-treated cells compared to vector or non-specific GFP shRNA control cells (Fig. 1B, panels II and III). The transcriptional activity of p53 is thought to be important for its functions in cell growth regulation, so luciferase activity was measured after treatment with AE in p53-knockdown cells that were co-transfected with a p53-luc plasmid (which contains three p53 binding sites upstream of the luciferase gene) or a p21-luc plasmid (which contains three p21 binding sites upstream of the luciferase gene) and an expression plasmid encoding wt, mutant p53 (R248W), or p53 (R175H). The p53 and p21 promoter-driven luciferase activities increased markedly in cells co-transfected with wt p53 but not in those co-transfected with p53 (R248W) or p53 (R175H), and

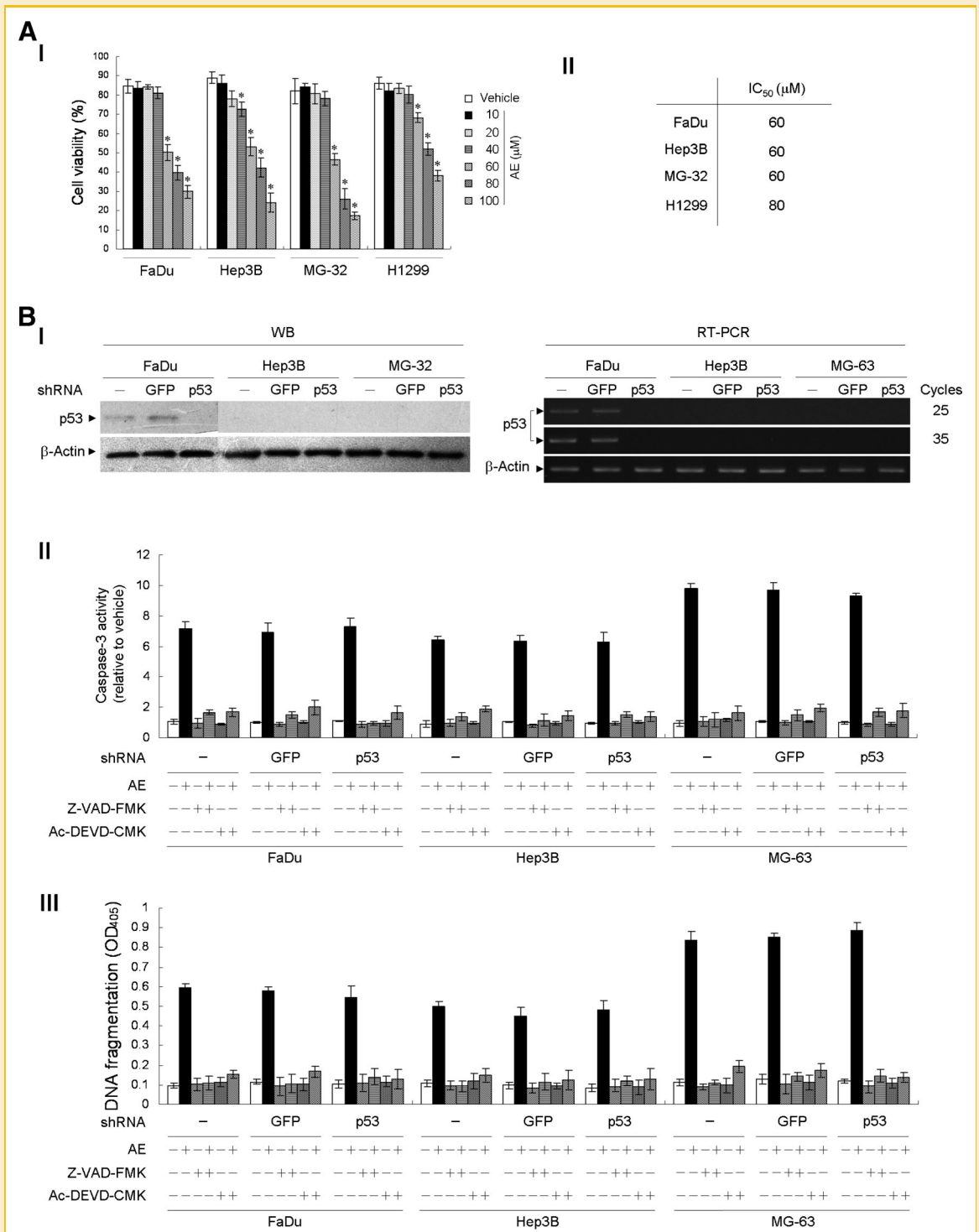

Fig. 1. AE induces apoptotic cell death in a p53-independent manner. A: The effect of AE on cell viability. FaDu, Hep3B, MG-32, or H1299 cells were plated in 24-well plates and treated with either DMSO (vehicle control) or the indicated concentrations of AE for 36 h (panel I). After treatment, cell viability was determined by flow-cytometric analysis of PI uptake. The values presented are the mean ± standard error from three independent experiments. $^{*}P < 0.05$, significantly different from vehicle-treated cells. The IC_{50} value of AE in these cells is indicated (panel II). B: p53 is not involved in the induction of apoptotic cell death or of caspase-3 activity by AE. Panel I: Levels of p53 proteins determined by Western blot analysis with p53 antibodies (left) and levels of p53 transcripts determined by RT-PCR with specific primers (right) in cells stably expressing the empty control vector (–), GFP shRNA, or p53 shRNA. β-Actin was used as an internal control for sample loading. Panels II and III: After treatment of the empty control vector (–), GFP shRNA, and p53 shRNA cells with vehicle, AE (60 μM), AE (60 μM) plus Ac-DEVD-CMK (10 μM), or AE (60 μM) plus Z-VAD-FMK (15 μM) for 36 h, caspase-3 activity and DNA fragmentation were determined using flow cytometry and cell death-detection ELISA, respectively. The values presented in panels I and II are the mean ± standard error from three independent experiments.

AE treatment did not reduce this increase in activity (Fig. 2A,B, comparing column 3 with column 4). In contrast, growth inhibition was observed in wt p53-, p53 (R248W)-, or p53 (R175H)-expressing cells treated with AE (Fig. 2C, columns 4, 6, and 8). The expression and promoter activity of p21, however, were increased in AE-treated cells co-transfected with control vector, p53 (R248W), or p53 (R175H) (Fig. 2C,D, columns 2, 6, and 8). These results clearly indicate that induction of both apoptotic cell death and p21 expression by AE occur independently of p53 expression.

FORMATION OF CYCLIN A–CdK2–p21 COMPLEXES IS ASSOCIATED WITH S-PHASE CELL CYCLE ARREST BY AE

To gain insight into the mechanism responsible for cell growth inhibition by AE, flow cytometry was used to determine the effect of AE on the cell cycle profile. With AE treatment, more p53 shRNA cells accumulated in S-phase than GFP shRNA control cells (Table I). A significant increase in the number of apoptotic cells (sub-G_1-phase population) was also observed in AE-treated cells expressing either p53 shRNA or non-specific GFP shRNA control (Table I). AE did not affect the level of cyclin B1, cyclin D, or cyclin E, but it did increase cyclin A and E2F1 expression as well as the phosphorylation of Cdk2 (Thr14/Thr15) (Fig. 3A, panel I). A co-immunoprecipitation assay was performed in p53 shRNA cell extracts using antibodies specific for Cdk2 and cyclin A to characterize the effect of AE on the interaction between cyclin A and Cdk2. As expected, AE induced the binding of cyclin A to Cdk2. Western blot analysis also showed that p21 was associated with the cyclin A–Cdk2 complex after AE treatment (Fig. 3B, panel II). However, PCNA and E2F1 were not detected in cyclin A–Cdk2 complexes. To further investigate whether the increase in cyclin A expression was associated with AE-induced cell cycle arrest at S-phase, p53 shRNA cells were transfected with cyclin A siRNA, which inhibited the expression of cyclin A and AE-induced S-phase arrest (panels I and II, respectively, of Fig. 3B). These results indicate that AE inhibited mutant p53-expressing or p53-null cancer cell growth through cell cycle arrest at S-phase, which was associated with the formation of cyclin A–Cdk2–p21 complexes.

INVOLVEMENT OF ERK ACTIVATION IN THE INDUCTION OF p21 AND E2F1 EXPRESSION, S-PHASE ARREST, AND APOPTOSIS BY AE

We examined the activation of MAP kinases, which are important regulators of p21 in the p53-independent pathway, to explore the mechanism underlying AE-induced p21 expression. Treatment with AE induced the phosphorylation of ERK, which was greatly reduced by the ERK inhibitor PD98059 and was attenuated by ERK-specific siRNA (Fig. 4A). Nevertheless, AE treatment did not result in the activation of p38 MAPK or JNK (data not shown). The induction of p21 and E2F1 expression, phosphorylation of ERK, and growth arrest were correlated with ERK activity, because addition of PD98059 or ERK-specific siRNA suppressed AE-induced p21 and E2F1 expression, ERK phosphorylation, and S-phase arrest (Fig. 4A,B, panel I). AE-induced apoptosis was, however, only partially suppressed by PD98059 or ERK-specific siRNA (Fig. 4B, panel II). Thus, these results suggest that the activation of ERK is required for AE-induced p21 and E2F1 expression and S-phase arrest and is involved in the induction of apoptosis.

INVOLVEMENT OF Bcl-X_L AND BAX EXPRESSION IN AE-INDUCED APOPTOTIC CELL DEATH

We evaluated the expression of anti- and pro-apoptotic Bcl-2 family proteins exposed to AE to further define the apoptotic pathway that is associated with AE treatment. Western blot analysis showed that Bcl-2 expression did not change, whereas expression of Bcl-X_L was markedly inhibited by AE (Fig. 5A, panel I). Heterodimerization of Bcl-X_L and Bax appears to be required for anti-apoptotic activity, and the susceptibility of cells to the induction of apoptosis may be regulated by the ratio of Bcl-X_L to Bax [Sedlak et al., 1995]. Accordingly, we determined the level of Bax expression. As expected, AE treatment led to an up-regulation of Bax expression (Fig. 5A, panel II). In contrast, Bak and MCL-1 levels were unaffected by AE (data not shown). We next examined the effect of AE on the expression of the inactivator BH3 and activator BH3 proteins, which regulate the activation of Bax/Bak [Galonek and Hardwick, 2006]. The expression of the inactivator BH3 proteins Bad, Bik, and NOXA did not change after AE treatment (data not shown). Similarly, no changes were observed in the expression of activator BH3 proteins BIM and PUMA; however, an increase in the amount of cleaved tBid was detected in AE-treated cells (Fig. 5A, panel II).

To clarify whether AE induces apoptotic cell death through changes in Bcl-X_L and Bax expression, transient ectopic FLAG-tagged Bcl-X_L or Bcl-2 was expressed in cells, and the expression of Bax and Bak was attenuated with siRNAs. Expression levels of Bcl-X_L, Bcl-2, Bax, and Bak were confirmed by Western blotting using FLAG-, Bax-, and Bak-specific antibodies (panels I and II of Fig. 5B). Compared with control vector-transfected cells, ectopic expression of Bcl-X_L (but not of Bcl-2) significantly suppressed AE-induced apoptosis (Fig. 5B, panels III and IV, compare column 4 with column 6). Furthermore, siRNA-mediated attenuation of Bax (but not of Bak) abolished PARP cleavage and apoptosis induction (Fig. 5C, panels I–III). These results demonstrate that changes in Bcl-X_L and Bax expression are involved in AE-induced apoptotic cell death.

INVOLVEMENT OF CASPASE-8 ACTIVATION IN THE AE-INDUCED LOSS OF $\Delta\psi_M$, INCREASES IN ROS AND Ca^{++} LEVELS, ERK PHOSPHORYLATION, CASPASE-9 ACTIVATION, AND APOPTOTIC DEATH

Bcl-X_L is localized to the outer mitochondrial membrane and regulates the $\Delta\psi_m$ [Breckenridge and Xue, 2004]. Therefore, we examined whether $\Delta\psi_m$ loss occurs in AE-treated cells. AE treatment for 1 h caused a rapid decrease in $\Delta\psi_m$, and the reduction in $\Delta\psi_m$ was maintained for up to 12 h of AE exposure (Fig. 6A, panel I). The alteration of $\Delta\psi_m$ was completely inhibited by CsA and the caspase-8 inhibitor Z-IETD-FMK (Fig. 6A, panel I). We next investigated whether AE treatment affects the levels of cytosolic ROS and Ca^{++}. Levels of ROS and Ca^{++} in the cytosol, which were determined by flow cytometry, increased in cells after treatment with AE, and these elevated levels were maintained throughout the 12-h exposure (Fig. 6A, panels II and III). Co-treatment with Z-IETD-FMK or CsA completely inhibited the increase in ROS and Ca^{++} caused by AE

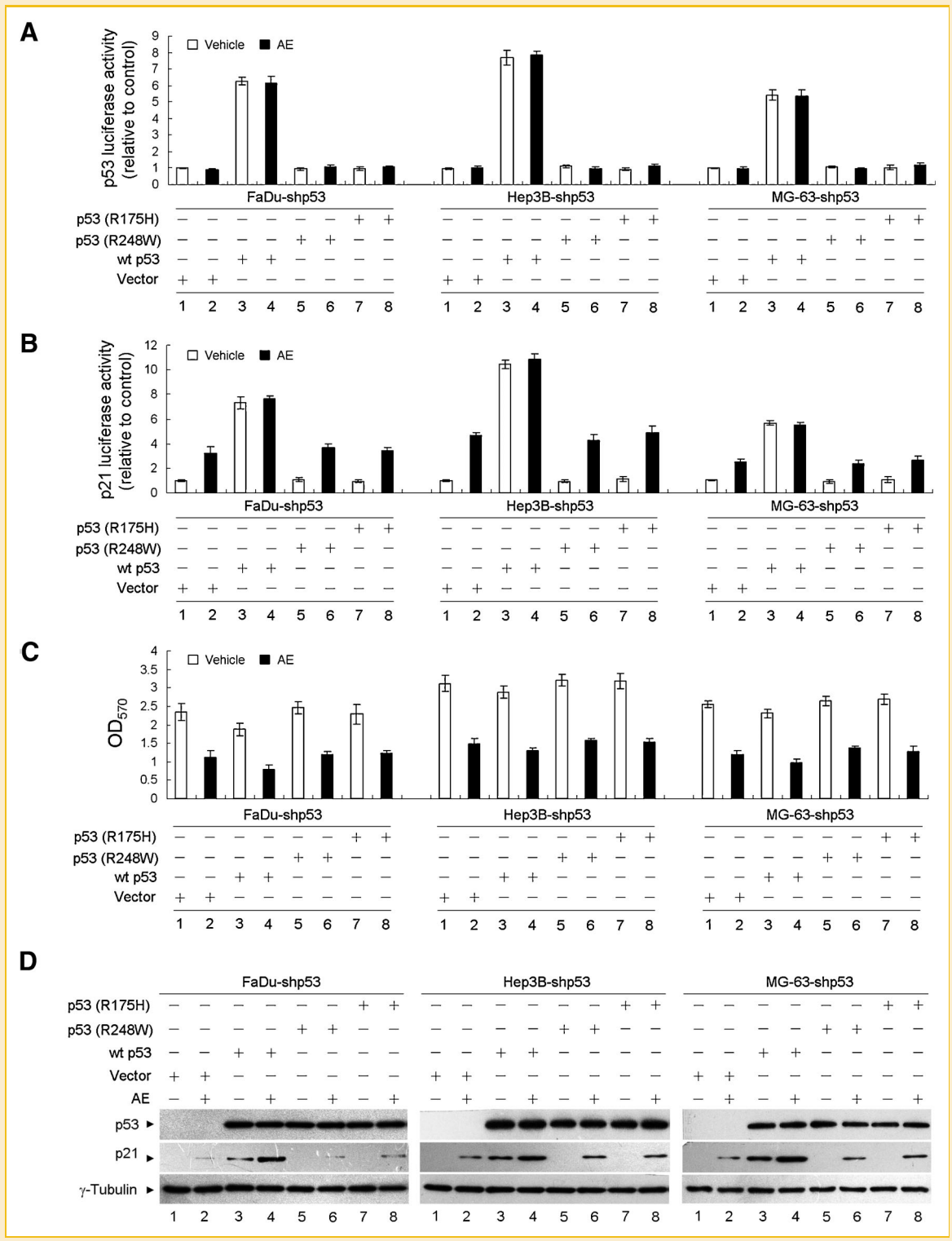

Fig. 2. p53 activity is not involved in the induction of cell death or of p21 activity. A: A luciferase reporter driven by three p53-binding sites was co-transfected with vector alone (lanes 1 and 2), wt p53 (lanes 3 and 4), mutant p53 (R248W) (lanes 5 and 6), or mutant p53 (R175H) (lanes 7 and 8) into stably p53 shRNA-expressing cells. B: As in (A), except that the reporter was driven by the p21 promoter. At 12 h post-transfection, cells were treated with vehicle or AE (60 μM) for 24 h, and then luciferase activity was determined. C,D: p53 shRNA-expressing stable cells were transfected with vector alone (lanes 1 and 2), wt p53 (lanes 3 and 4), mutant p53 (R248W) (lanes 5 and 6), or mutant p53 (R175H) (lanes 7 and 8) for 12 h. Cells were then treated with either vehicle or AE (60 μM) for 24 h. Cell viability and protein expression were determined using the MTT assay and Western blot analysis, respectively. γ-Tubulin was used as an internal control for sample loading in panel IV.

TABLE I. Effect of AE on the Cell Cycle Progression of p53-Deficient Tumor Cell Lines

		Cell cycle phase (% of cells)							
		G_1		S		G_2/M		Sub-G_1	
Time	Cell line	Vehicle	AE	Vehicle	AE	Vehicle	AE	Vehicle	AE
24 h	FaDu								
	shGFP	44.2 ± 3.1	25.8 ± 5.2*	46.8 ± 4.2	59.2 ± 2.8*	8.8 ± 3.9	14.4 ± 3.2	0.6 ± 0.1	12.4 ± 2.3
	shp53	43.9 ± 4.3	25.0 ± 3.1*	45.6 ± 2.2	61.8 ± 3.9*	9.9 ± 1.5	13.5 ± 2.2	0.6 ± 0.2	14.7 ± 3.2
	Hep3B								
	shGFP	48.8 ± 4.2	18.1 ± 4.3*	43.3 ± 3.9	67.8 ± 6.1*	7.8 ± 2.5	14.2 ± 5.0	0.3 ± 0.1	10.2 ± 2.1
	shp53	49.1 ± 5.7	19.4 ± 2.1*	41.2 ± 5.1	65.9 ± 3.8*	9.7 ± 3.5	15.2 ± 3.1	0.3 ± 0.1	12.7 ± 2.6
	MG-63								
	shGFP	40.7 ± 3.9	20.4 ± 3.8*	44.2 ± 2.1	61.3 ± 5.1*	15.1 ± 2.4	18.3 ± 2.2	0.3 ± 0.1	20.2 ± 1.9
	shp53	41.9 ± 5.3	24.4 ± 2.8*	44.6 ± 3.1	58.7 ± 2.2*	13.4 ± 2.9	16.9 ± 3.7	0.4 ± 0.1	19.6 ± 3.4
48 h	FaDu								
	shGFP	62.3 ± 4.2	29.1 ± 4.8*	32.6 ± 2.5	62.4 ± 2.6*	5.4 ± 2.2	7.9 ± 3.7	0.9 ± 0.3	30.2 ± 4.2
	shp53	63.4 ± 5.2	27.6 ± 3.1*	31.6 ± 3.1	64.7 ± 4.7*	4.9 ± 2.7	8.6 ± 3.2	0.7 ± 0.2	28.9 ± 2.5
	Hep3B								
	shGFP	59.3 ± 2.8	11.8 ± 4.3*	26.8 ± 2.2	76.8 ± 4.3*	13.5 ± 2.1	11.7 ± 5.2	1.1 ± 0.3	17.5 ± 3.0
	shp53	56.9 ± 5.1	12.3 ± 2.9*	30.6 ± 4.1	78.6 ± 3.6*	12.6 ± 4.1	9.4 ± 2.9	0.9 ± 0.2	19.2 ± 3.7
	MG-63								
	shGFP	68.4 ± 2.2	18.4 ± 2.9*	23.6 ± 3.8	72.2 ± 3.9*	8.0 ± 1.1	9.4 ± 1.1	0.9 ± 0.2	39.3 ± 3.8
	shp53	70.1 ± 5.7	16.5 ± 4.1*	24.1 ± 4.1	75.2 ± 2.7*	5.8 ± 3.5	8.3 ± 2.8	1.3 ± 0.5	37.1 ± 4.6

The values presented are the mean ± standard errors from three independent experiments.
*$P < 0.05$, significantly different from vehicle-treated cells.

(Fig. 6A, panels II and III). The AE-induced increase in cytosolic Ca^{++} was, however, unaffected by the addition of dantrolene, an inhibitor of Ca^{++} release from the endoplasmic reticulum (Fig. 6A, panel III), indicating that the increase in cytosolic Ca^{++} was due to release from mitochondria. Interestingly, apoptosis was also prevented by co-treatment with Z-IETD-FMK or with Z-IETD-FMK and PD98059 (Fig. 6A, panel IV). Additionally, AE-induced Bax expression, Bid cleavage, translocation of tBid to the mitochondria, and ERK phosphorylation were inhibited by co-treatment with Z-IETD-FMK (Fig. 6B), suggesting that induction of Bax and cleavage of Bid are dependent on the activation of caspase-8. These results suggest that caspase-8 activation is involved in the AE-induced loss of $\Delta\psi_m$, increase in cytosolic ROS and Ca^{++} levels, ERK phosphorylation, and apoptosis.

To investigate whether caspase-9 activity is involved in the induction of apoptosis, the caspase-9-specific inhibitor Z-LEHD-FMK was used. AE-mediated activation of caspase-9 was inhibited by Z-LEHD-FMK and Z-IETD-FMK but not by treatment with the caspase-4 inhibitor LEVD-CHO (Fig. 6C, panel I). AE-induced apoptosis was only partially inhibited by PD98059, but it was completely inhibited by either Z-IETD-FMK or Z-LEHD-FMK (Fig. 6C, panel II). These data indicate that AE-induced apoptosis requires caspase-8-mediated activation of the mitochondrial death pathway and ERK signaling.

INVOLVEMENT OF CASPASE-8 ACTIVATION IN THE AE-INDUCED RELEASE OF CYTOCHROME C, AIF, AND ENDO G FROM MITOCHONDRIA

Western blot analysis was conducted to investigate whether AE treatment induces the mitochondrial release of pro-apoptotic proteins. AE induced the release of cytochrome *c*, AIF, and Endo G into the cytosol. The release of cytochrome *c*, AIF, and Endo G was, however, completely inhibited by Z-IETD-FMK (Fig. 6D, panels I–III). Therefore, caspase-8 initiates the AE-induced release of cytochrome *c*, AIF, and Endo G, in addition to initiating apoptotic cell death.

DIMINISHING THE STABILITY OF CARP1 AND 2 mRNAs BY AE CONTRIBUTES TO INDUCTION OF CASPASE-8 ACTIVITY AND CELL DEATH

We next tested whether the suppression of CARPs contributes to the activation of caspase-8 in response to AE, as CARPs have previously been shown to regulate the activity of caspase-8 [McDonald and El-Deiry, 2004]. Treatment with AE for 1 h reduced the expression of *CARP1* and *2* mRNAs, and this reduction in both mRNAs was maintained for up to 12 h of AE exposure (Fig. 7A). By using actinomycin D (a transcriptional inhibitor) and cycloheximide (a translational inhibitor), we observed that decreased CARP mRNA levels by AE was related to reduced stabilization of the mRNAs. To extend the above observations, we tested whether the ectopic expression of FLAG-tagged CARP1 or 2 leads to the suppression of caspase-8 activity and apoptosis. Expression levels of FLAG-CARP1 and -2 were confirmed by Western blotting using FLAG-specific antibody (Fig. 7B, panel I). As shown in panels II and III of Figure 7B, AE-induced increases of caspase-8 activity and apoptosis were inhibited in the CARP1- or CARP2-transfected cells compared with control vector-transfected cells. Because the overexpression of CARPs can contribute to the ubiquitin-mediated proteolysis of caspase-8 [McDonald and El-Deiry, 2004], we then investigated whether CARP overexpression affects the levels of caspase-8 protein. As expected, pro-caspase-8 protein levels were reduced when FLAG-CARP1 or FLAG-CARP2 was transfected in cells (Fig. 7B, panel I), whereas pro-caspase-10 protein levels were partially affected. In contrast, overexpression of FLAG-CARPs did not affect levels of pro-caspase-9 protein. Taken together, these data demonstrate that the decrease of CARPs is required for caspase-8 activation and apoptosis induction in response to AE.

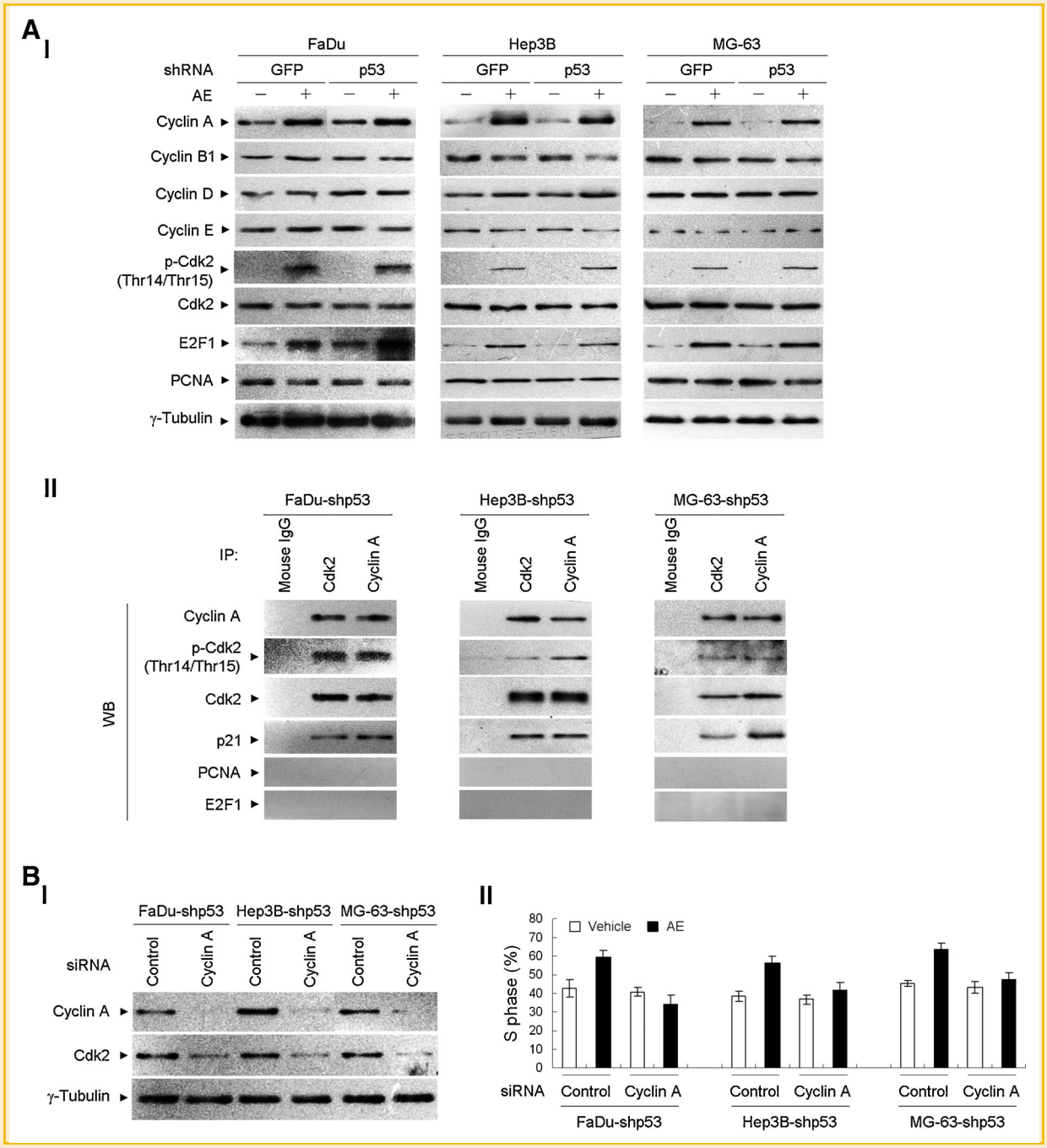

Fig. 3. Involvement of cyclin A–Cdk2–p21–E2F1 complexes in AE-induced S-phase cell cycle arrest. A: Effects of AE on cyclin protein expression and the levels of cyclin A, p21, and E2F1 bound to Cdk2. Panel I: After 36 h of treatment of the GFP shRNA- or p53 shRNA-expressing cells with vehicle or AE (60 μM), the levels of cyclin A, cyclin B1, cyclin D, cyclin E, Cdk2, p-Cdk2 (Thr14/Thr15), E2F1, and PCNA in the cell lysates were analyzed using specific antibodies. γ-Tubulin was used as an internal control for sample loading. Panel II: Co-immunoprecipitation of cyclin A, Cdk2, and p21 was performed using lysates prepared from AE (60 μM)-treated p53 shRNA-expressing stable cells at 36 h. The antibody used for co-immunoprecipitation is indicated at the top. The proteins in the immunoprecipitated complexes were detected using Western blotting with specific antibodies. Mouse normal IgG was used as a control for antibody specificity. B: At 12 h after transfection of p53 shRNA-expressing cells with control or cyclin A siRNA, cells were treated with either vehicle or AE (60 μM) for 24 h. After WB was used to examine the cyclin A and Cdk2 levels, the percentage of cells in S-phase was analyzed by flow-cytometric analysis of PI-stained cells.

DISCUSSION

In this study, we used the mutant p53 (R248L)-carrying cell line and the p53-null human lung cancer cell lines H1299, Hep3B, and MG-63 to explore the mechanism of p53-independent apoptosis induced by AE. Transient ectopic expression of wt p53, a p53- and p21-dependent luciferase reporter assay, and quantitative analyses of DNA fragmentation and caspase-8 activity in the presence of

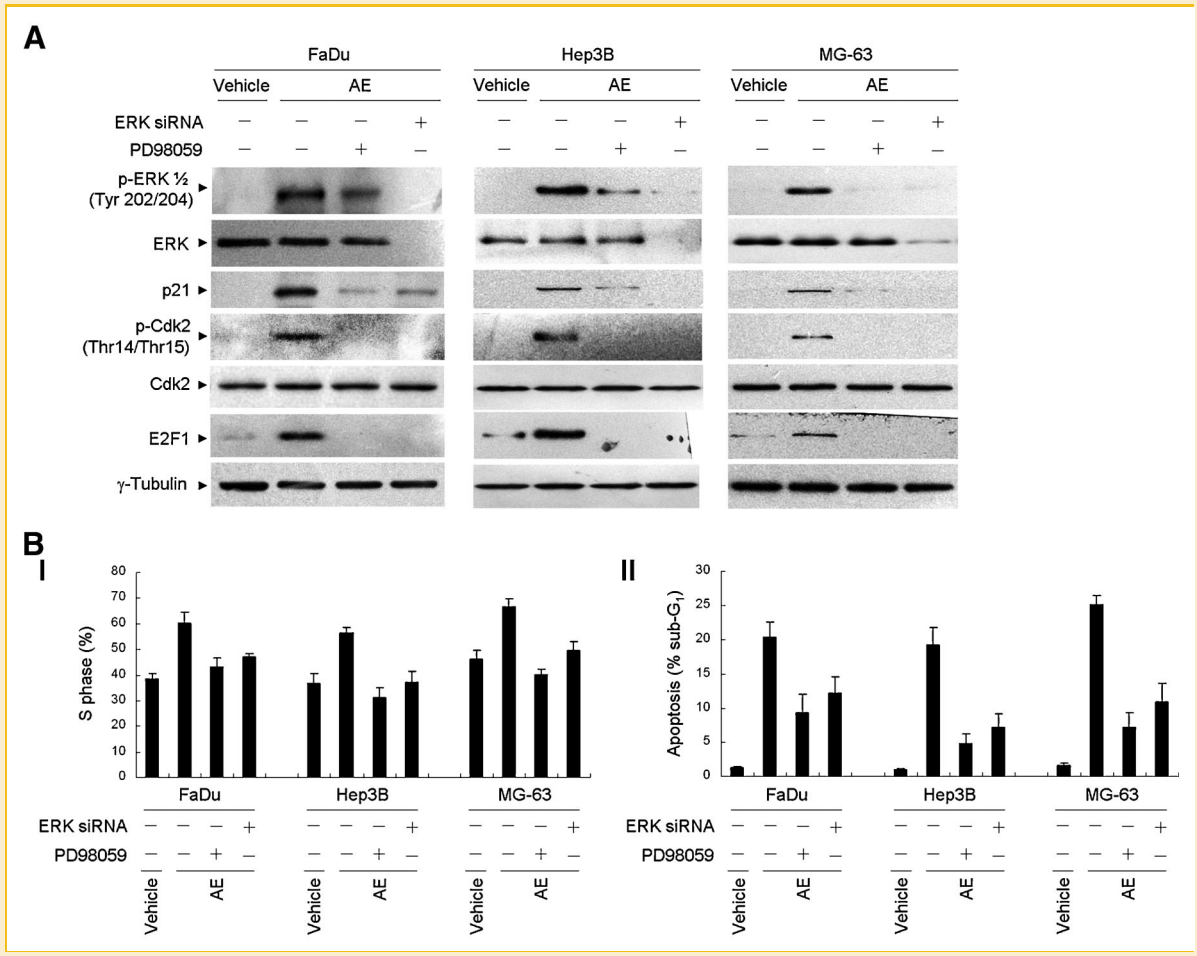

Fig. 4. Activation of ERK is involved in the induction of p21 and E2F1 expression, S-phase arrest, and apoptosis. At 12 h after transfection with ERK siRNA (pKD-MAPK1/Erk) or 2 h after treatment with PD98059, cells were treated with either vehicle or AE (60 μM) for 24 h. A: The levels of ERK, p-ERK (Tyr202/204), p21, and E2F1 in the cell lysates were then determined by Western blotting using specific antibodies. γ-Tubulin was used as an internal control for sample loading. B: The cell cycle profile and fraction of apoptotic cells (sub-G_1 phase population) were determined using flow cytometry. The values presented are the mean ± standard error from three independent experiments.

Z-IETD-FMK confirmed the induction of apoptotic cell death by AE through a caspase-8-dependent but p53-independent pathway. Furthermore, CARP proteins appear to be a crucial regulator activation of caspase-8 in response to AE, since overexpression of CARP1 and 2 reduced AE-induced caspase-8 activation and apoptosis. AE contains a quinine structure that is predicted to induce ROS production, which may play a role in the induction of cancer cell apoptosis [Lee et al., 2006]. AE displays an affinity for nuclear DNA, and high doses of AE disrupt chromatin structure and DNA template function in susceptible cell lines [Mueller and Stopper, 1999]. The participation of ROS in cancer cell apoptosis that is stimulated by chemotherapeutic agents through the induction of DNA damage has been investigated for several decades [Lau et al., 2008]. Oxidative damage to DNA is a result of the interaction of DNA with ROS. Consistent with previously reported results [Lee et al., 2006], an increase in intracellular ROS levels was observed when cells were induced to undergo apoptosis. ERK has been implicated in DNA damage-induced p53-independent apoptosis, and its activation is regulated by ROS [Wang et al., 1998]. We found that AE caused an increase in ROS levels that was completely inhibited by co-treatment with Z-IETD-FMK or CsA. The phosphorylation of ERK induced by AE was suppressed by Z-IETD-FMK. Moreover, PD98058 and ERK siRNA significantly attenuated the AE-induced expression of p21 and S-phase arrest, suggesting that ERK activation is correlated with AE-mediated p21 induction and S-phase arrest. Our results are in agreement with a previous report that activated ERK induces p21 expression in a p53-independent manner and that p21 up-regulation results in S-phase arrest [Zhu et al., 2004].

p21 inhibits the phosphorylation of Rb by the cyclin A–Cdk2 complex, which regulates the transition of G_1 to S-phase [Harper et al., 1993]. p21 also inhibits DNA synthesis and cell growth by binding to PCNA and Cdk2 with its N- and C-terminal regions, respectively [Rousseau et al., 1999]. The association of p21 with cyclin A–Cdk2 complexes was detected 12–48 h after AE treatment. Attenuating the activation of ERK with PD98059 or ERK siRNA significantly inhibited the expression of p21 and partially inhibited apoptosis induced by AE. Overexpression of p21 inhibits TRAIL death receptor DR4-dependent caspase-8 activation [Xu and El-Deiry, 2000]. An analysis using chimeric caspase-8 with the transmembrane and extracellular domains of the human CD8α

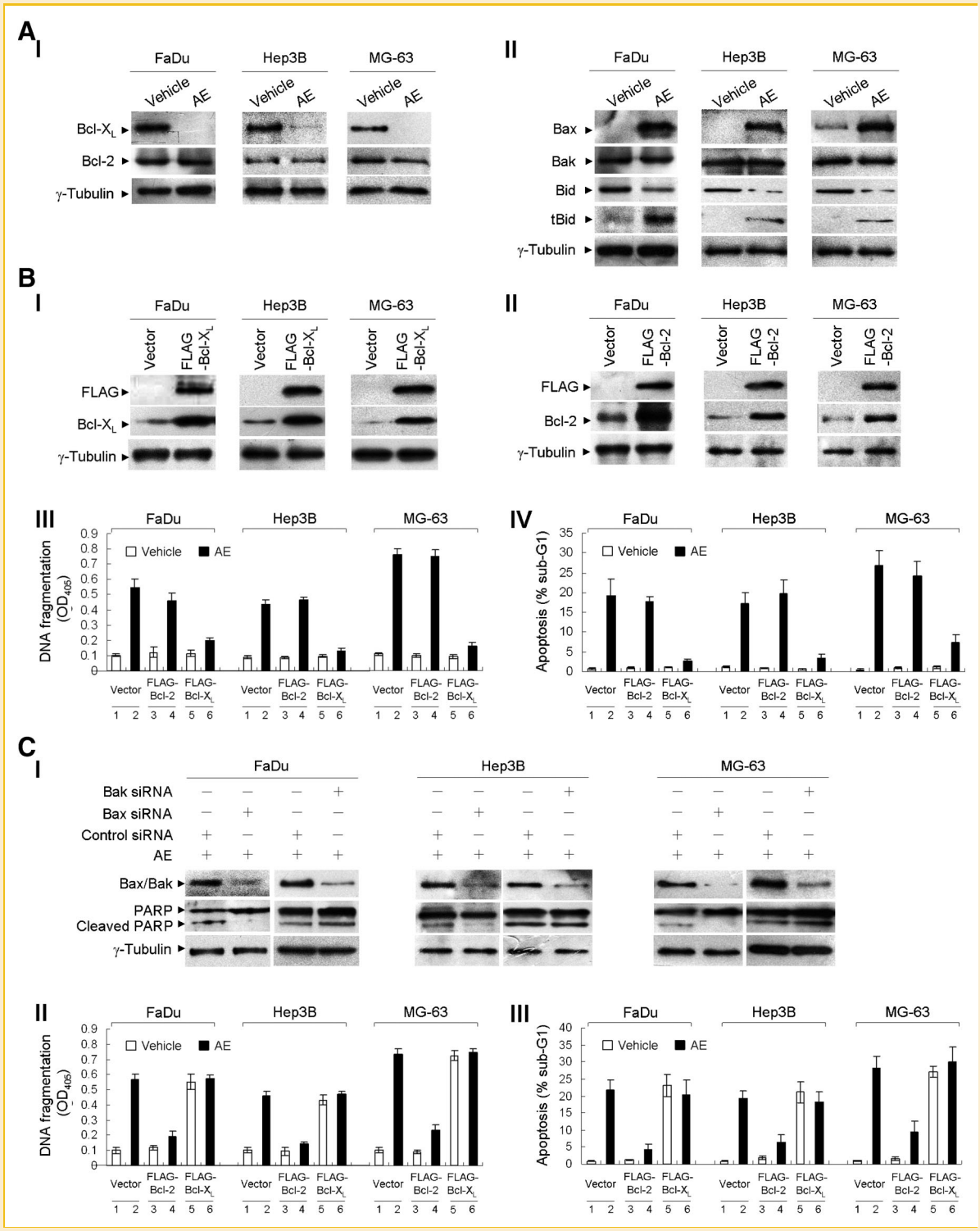

Fig. 5. Changes in Bcl-X_L and Bax expression are involved in AE-induced apoptosis. A: The effect of AE on the expression of Bcl-2 family proteins. The levels of Bcl-X_L, Bcl-2, Bax, Bak, Bid, and tBid in cell lysates prepared after 36 h of treatment with vehicle or AE (60 μM) were analyzed using specific antibodies (panels I and II). γ-Tubulin was used as an internal control for sample loading. B: Ectopic expression of Bcl-X_L suppresses AE-induced apoptosis. At 12 h after transfection with a FLAG-tagged Bcl-X_L or Bcl-2 expression construct, cells were treated with vehicle or AE (60 μM) for 24 h. Panel I: Expression levels of Bcl-X_L in lysates prepared from cells transfected with vector alone, FLAG-Bcl-X_L, or FLAG-Bcl-2. FLAG-Bcl-X_L, FLAG-Bcl-2, Bcl-X_L, and Bcl-2 were detected with the antibodies shown. C: Bax siRNA suppresses AE-induced apoptosis and PARP cleavage. At 12 h after transfection with control siRNA, Bax siRNA, or Bak siRNA, cells were treated with vehicle or AE (60 μM) for 24 h. Panel I: The levels of Bax, Bak, and PARP in the cell lysates were determined by Western blotting using specific antibodies. γ-Tubulin was used as an internal control for sample loading. Panels II and III (B,C): DNA fragmentation and the fraction of apoptotic cells (sub-G_1 phase population) were determined using cell death-detection ELISA and flow cytometry, respectively. The values presented are the mean ± standard error from three independent experiments.

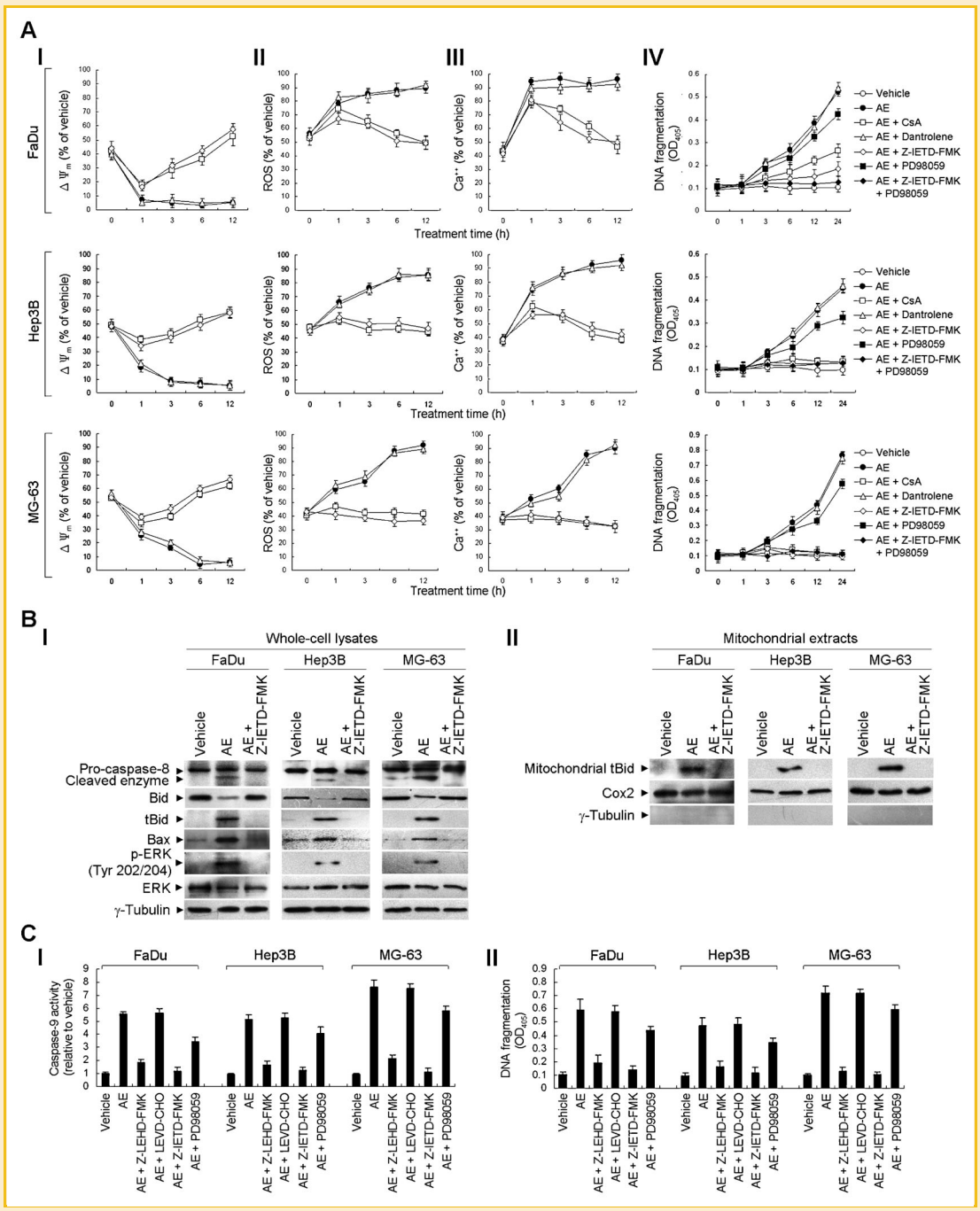

Fig. 6. Caspase-8 activation is involved in AE-induced $\Delta\psi_m$ loss, increases in cytosolic ROS and Ca^{++} levels, ERK phosphorylation, caspase-9 activation, apoptosis, and the release of cytochrome c, AIF, and Endo G from mitochondria. A: AE-induced changes in the levels of $\Delta\psi_m$, Ca^{++}, and ROS. At the indicated times, cells treated with vehicle, AE (60 μM), AE (60 μM) plus CsA (5 μM), AE (60 μM) plus Z-IETD-FMK (40 μM), AE (60 μM) plus dantrolene (25 μM), AE (60 μM) plus PD98059 (15 μM), or AE (60 μM) plus PD98059 (15 μM), and Z-IETD-FMK (40 μM) were harvested for the measurement of $\Delta\psi_m$, ROS, Ca^{++}, and DNA fragmentation. Panel I: The decrease in $DiOC_6$ fluorescence was measured by flow cytometry. Panels II and III: The generation of ROS and the cytosolic level of Ca^{++} were monitored by measuring increased fluorescence of Indo-1 and 2,7-dichlorodihydrofluorescein diacetate (DCF), respectively, by flow cytometry. Panel IV: DNA fragmentation was determined using cell death-detection ELISA. B: Z-IETD-FMK suppresses AE-induced Bax activation, Bid cleavage, translocation of tBid to the mitochondria, and ERK phosphorylation. The levels of caspase-8, Bax, Bid, tBid, ERK, and p-ERK (Tyr202/204) in whole-cell lysates (panel I) or tBid in mitochondrial extracts (panel II) were detected after 24 h of treatment with vehicle, AE (60 μM), or AE (60 μM) plus Z-IETD-FMK (40 μM). γ-Tubulin and Cox2 were measured as internal controls for whole cells and mitochondria, respectively. C: Caspase-8 is involved in the induction of caspase-9 and -3 activities. Cells were treated with vehicle, AE (60 μM), AE (60 μM) plus Z-LEHD-FMK (30 μM), AE (60 μM) plus LEVD-CHO (40 μM), AE plus Z-IETD-FMK (40 μM), or AE (60 μM) plus PD98059 (15 μM) for 36 h. Panels I and II: Caspase-9 activity and DNA fragmentation were determined using flow cytometry and cell death-detection ELISA, respectively. The values presented are the mean ± standard error from three independent experiments. D: Caspase-8 activation is involved in the release of cytochrome c, AIF, and Endo G from mitochondria in AE-treated cells. Cells were treated with vehicle, AE (60 μM), or AE (60 μM) plus Z-IETD-FMK (40 μM) for 36 h, and the levels of cytochrome c (panel I), AIF (panel II), and Endo G (panel III) in the cytosol and mitochondria were determined by Western blotting using specific antibodies. γ-Tubulin and Cox2 were determined as internal controls for whole cells and mitochondria, respectively.

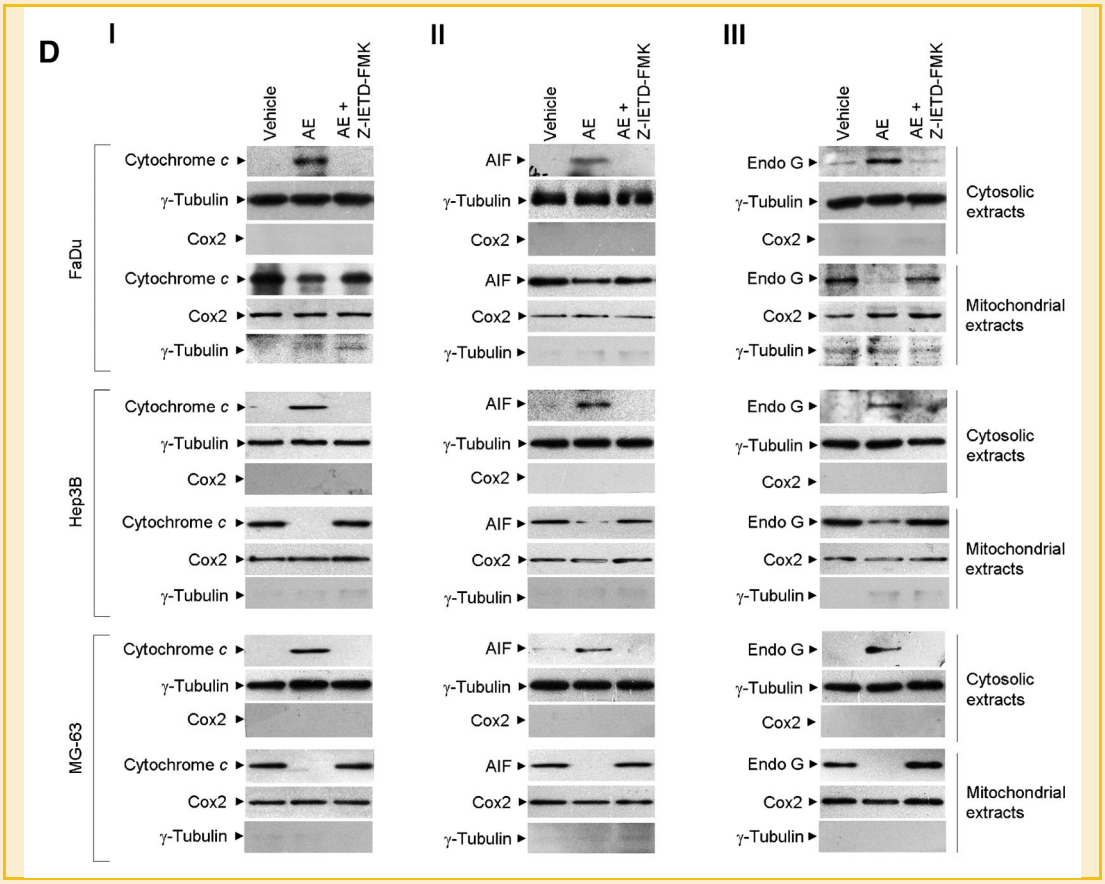

Fig. 6. (*Continued*)

chain did, however, demonstrate that caspase-8 oligomerization at the cell membrane is sufficient for its autoactivation and apoptosis induction [Martin et al., 1998]. Several chemotherapeutic agents, such as *N*,*N*-dimethyl phytosphingosine and curcumin, induce apoptosis through the cleavage of cytosolic Bid by activated caspase-8 [Anto et al., 2002; Kim et al., 2009]. Our results show that Z-IETD-FMK inhibited the cleavage and activation of caspase-8 and of apoptotic cell death induced by AE. The FaDu cell line has a homozygous deletion of the death receptor DR4 and is resistant to the cytotoxic effects of TRAIL [Ozoren et al., 2000]. Moreover, FADD siRNA did not interfere with the activation of caspase-8 in FaDu, Hep3B, or MG-63 cells treated with AE (data not shown), suggesting that AE-induced caspase-8 activation and apoptosis do not occur through the induction of the death receptor. The promoter region of caspase-8 contains an E2F1-responsive element, and its transcriptional activity can be regulated by E2F1 [Afshar et al., 2006]. Previous findings also show that radiation does not induce E2F1 activity, caspase-8 activity, or apoptotic cell death when cells express wt p53; however, inhibition of wt p53 function with HPV-16 E6 induces caspase-8 activity and apoptosis following radiation [Afshar et al., 2006]. Taken together, these observations led us to speculate that the caspase-8-dependent mitochondrial ROS production is critical for ERK activation and the subsequent p21 induction and E2F1 expression. The formation of cyclin A–Cdk2–p21 complexes induced by activated ERK after treatment with AE was associated with the induction of S-phase arrest, and E2F1 up-regulation may contribute to caspase-8 activation.

The release of cytochrome *c* from the mitochondrial intermembrane space to the cytosol in response to stress stimuli is a critical step for the activation of caspase-9 in apoptotic cell death [Tsujimoto, 2003]. In cultured dopaminergic PC12 cells, caspase-9 activation via cytochrome *c* release in response to 1-methyl-4-phenyl-1,2,3,6-tetrahydropyridine results in the activation of caspase-3 and -8 and the cleavage of Bid to tBid [Viswanath et al., 2001]. Our results show that either CsA or Z-IETD-FMK inhibited AE-induced loss of $\Delta\psi_m$ and apoptotic cell death. Co-treatment with Z-IETD-FMK also completely blocked Bid cleavage, the translocation of tBid to the mitochondria, Bax induction, caspase-9 activation, and apoptosis. Moreover, experiments using Z-IETD-FMK showed that caspase-8 activity appeared to be involved in the AE-induced release of cytochrome *c*, AIF, and Endo G from the mitochondria and apoptosis. Our findings suggest that caspase-9 was activated directly by caspase-8 through the release of cytochrome *c*.

CARPs act as ubiquitin protein ligases that bind to and regulate caspase-8 and -10. siRNA-mediated attenuation of CARP expression significantly sensitizes cells to chemotherapy-induced apoptosis and inhibits colony formation by cancer cells [McDonald and

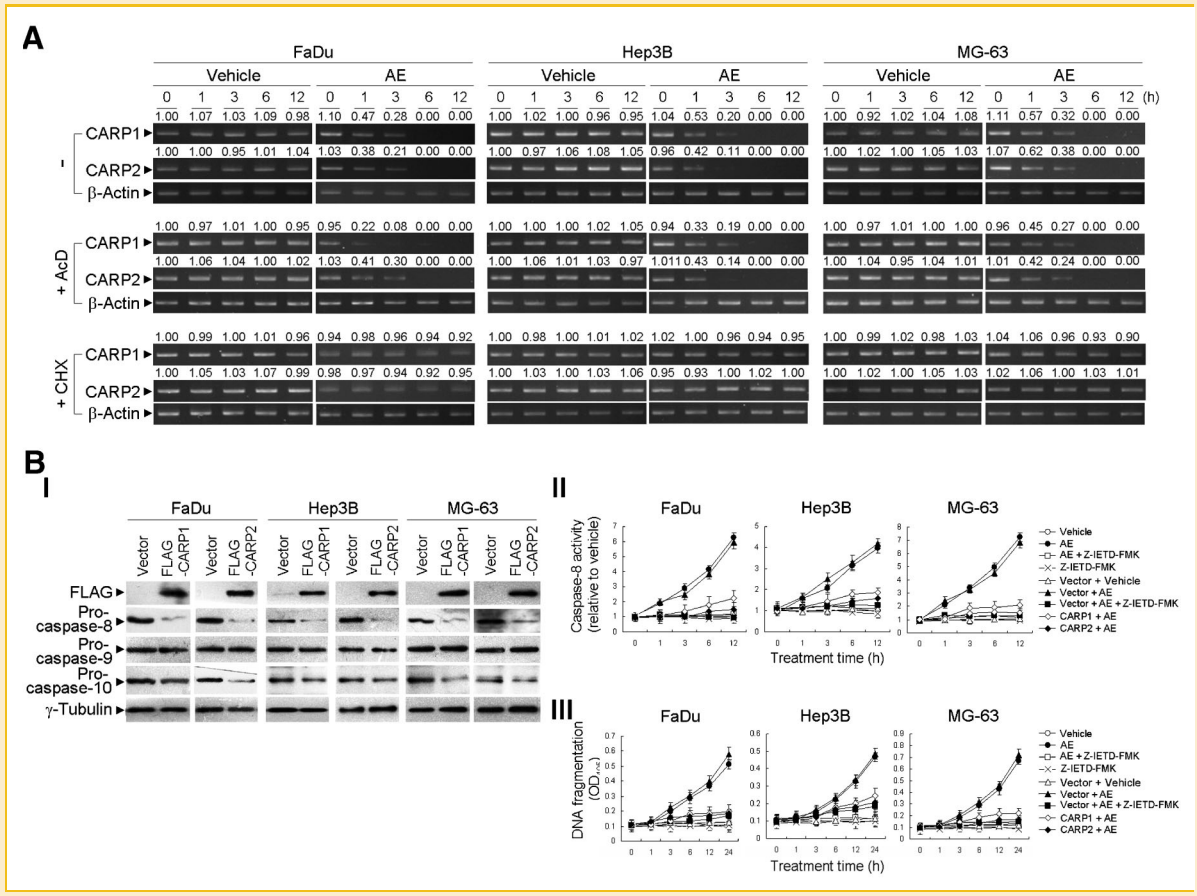

Fig. 7. AE induces caspase-8 activation and apoptosis by decreasing the stability of *CARP1* and *CARP2* mRNAs. A: RT-PCR reveals that the stability of *CARP1* and *CARP2* mRNAs was reduced in AE-treated cells. The cells were pre-incubated with 0.5 μg/ml of actinomycin D (AcD) or 2 μg/ml of cycloheximide (CHX) for 1 h, cells were then treated with vehicle or AE (60 μM) for the indicated periods. Total RNAs were reverse-transcribed and PCR-amplified using *CARP1*- or *CARP2*-specific primers. β-Actin was used as an internal control for sample loading. The values above the figures represent relative densities of the bands normalized to β-actin. B: Ectopic expression of CARP1 or CARP2 suppresses AE-induced caspase-8 activation and apoptosis. Panel I: Expression levels of Bcl-X_L in lysates prepared from cells transfected with vector alone, FLAG-CARP1, or FLAG-CARP2. FLAG-CARP1, FLAG-CARP2, pro-caspase-8, and pro-caspase-9 were detected with the antibodies shown. Panels II and III: At 12 h after transfection with vector alone, FLAG-CARP1, or FLAG-CARP2, cells were treated with vehicle, AE (60 μM) or AE (60 μM) plus Z-IETD-FMK (40 μM) for 24 h. Caspase-8 activity and DNA fragmentation were determined using flow cytometry and cell death-detection ELISA, respectively. The values presented are the mean ± standard error from three independent experiments.

El-Deiry, 2004]. In addition, treatment with TNF-α/cycloheximide or TRAIL leads to enhanced cleavage of caspase-8 and -10 after treatment with CARP1 or CARP2 siRNA. One study using a caspase-3 inhibitor or a combination of caspase-8 and -10 inhibitors and the proteasome inhibitor MG132 demonstrated that cleavage of CARPs was caspase-dependent during death receptor-mediated apoptosis [McDonald and El-Deiry, 2004]. CARPs are also overexpressed in a variety of human cancers and cancer cell lines, suggesting that CARPs could contribute to development of tumors [McDonald and El-Deiry, 2004]. However, resistance to chemotherapy-induced or death receptor-mediated apoptosis has not been observed in cells overexpressing CARP1 or CARP2. AE treatment of FaDu, Hep3B, and MG-32 cells led to the rapid decrease of both *CARP1* and *CARP2* mRNAs. Overexpression of either CARP1 or CARP2 blocked AE-induced caspase-8 activity and apoptosis as well as decreased the levels of pro-caspase-8 protein. Unexpectedly, pro-caspase-10 protein levels only slightly decreased in CARP1- or CARP2-overexpressing cells. The sequences of caspase-8 and -10 are highly similar [Fernandes-Alnemri et al., 1996]. The involvement of caspase-10 in apoptosis signaling by death receptors has also been reported [Wang et al., 2001]. However, in vitro experiments showed that overexpression of caspase-10 is able to induce the process of caspase-3 cleavage and apoptosis [Vincenz and Dixit, 1997]. Caspase-8-deficient cell lines were shown to be resistant toward Apo2L/TRAIL-induced apoptosis, implying that caspase-8 plays a critical role in death receptor-mediated signaling, whereas caspase-10 is not important for this function [Bodmer et al., 2000]. Interestingly, studies using a series of caspase-10-specific antibodies demonstrated that apoptosis signaling by death receptors involves not only caspase-8 but also caspase-10 [Kischkel et al., 2001]. If AE treatment induced apoptosis by increasing the activities of both caspase-8 and -10, the addition of an inhibitor of either caspase-8 or -10 would be predicted to result in decreased apoptosis. We found that apoptotic induction by AE was inhibited by caspase-8 inhibitor, but not by caspase-10 inhibitor. Furthermore, caspase-10 cleavage and activation were not detected in AE-treated cells (data not shown). These findings indicate that caspase-8 activation is an important event in induction of apoptosis by AE. These observations

together with our findings suggest that the function and regulation of both caspase-8 and -10 are independent of apoptosis induction. This raised the possibility that the two proteins have distinct and perhaps complementary functions.

In conclusion, we present a novel p53-independnet mechanism of AE-induced apoptosis of cancer cells involving decreased stability of CARP mRNAs and the subsequent induction of ERK and caspase-8-mediated mitochondrial death pathways. However, the molecular mechanisms of the diminished CARP mRNA stability in AE-treated cells remain to be further explored.

ACKNOWLEDGMENTS

M.-L. Lin was supported by a grant (CMU98-C-06) from China Medical University, Taiwan. S.-S. Chen was supported by grants from the Taichung Veterans General Hospital and Central Taiwan University of Science and Technology (TCVGH-CTUST987715), Taiwan.

REFERENCES

Afshar G, Jelluma N, Yang X, Basila D, Arvold ND, Karlsson A, Yount GL, Dansen TB, Koller E, Haas-Kogan DA. 2006. Radiation-induced caspase-8 mediates p53-independent apoptosis in glioma cells. Cancer Res 66:4223–4232.

Anto RJ, Mukhopadhyay A, Denning K, Aggarwal BB. 2002. Curcumin (diferuloylmethane) induces apoptosis through activation of caspase-8, BID cleavage and cytochrome c release: Its suppression by ectopic expression of Bcl-2 and Bcl-xl. Carcinogenesis 23:143–150.

Arnoult D, Gaume B, Karbowski M, Sharpe JC, Cecconi F, Youle RJ. 2003. Mitochondrial release of AIF and EndoG requires caspase activation downstream of Bax/Bak-mediated permeabilization. EMBO J 22:4385–4399.

Bodmer JL, Holler N, Reynard S, Vinciguerra P, Schneider P, Juo P, Blenis J, Tschopp J. 2000. TRAIL receptor-2 signals apoptosis through FADD and caspase-8. Nat Cell Biol 2:241–243.

Breckenridge DG, Xue D. 2004. Regulation of mitochondrial membrane permeabilization by BCL-2 family proteins and caspases. Curr Opin Cell Biol 16:647–652.

Brunelle JK, Letai A. 2009. Control of mitochondrial apoptosis by the Bcl-2 family. J Cell Sci 122:437–441.

Budihardjo I, Oliver H, Lutter M, Luo X, Wang X. 1999. Biochemical pathways of caspase activation during apoptosis. Annu Rev Cell Dev Biol 15:269–290.

Chao JI, Kuo PC, Hsu TS. 2004. Down-regulation of survivin in nitric oxide-induced cell growth inhibition and apoptosis of the human lung carcinoma cells. J Biol Chem 279:20267–20276.

Dhillon AS, Hagan S, Rath O, Kolch W. 2007. MAP kinase signalling pathways in cancer. Oncogene 26:3279–3290.

Fernandes-Alnemri T, Armstrong RC, Krebs J, Srinivasula SM, Wang L, Bullrich F, Fritz LC, Trapani JA, Tomaselli KJ, Litwack G, Alnemri ES. 1996. In vitro activation of CPP32 and Mch3 by Mch4, a novel human apoptotic cysteine protease containing two FADD-like domains. Proc Natl Acad Sci USA 93:7464–7469.

Galonek HL, Hardwick JM. 2006. Upgrading the BCL-2 network. Nat Cell Biol 8:1317–1319.

Harper JW, Adami GR, Wei N, Keyomarsi K, Elledge SJ. 1993. The p21 Cdk-interacting protein Cip1 is a potent inhibitor of G1 cyclin-dependent kinases. Cell 75:805–816.

Hill CS, Treisman R. 1995. Transcriptional regulation by extracellular signals: Mechanisms and specificity. Cell 80:199–211.

Kim BM, Choi YJ, Han Y, Yun YS, Hong SH. 2009. N,N-dimethyl phytosphingosine induces caspase-8-dependent cytochrome c release and apoptosis through ROS generation in human leukemia cells. Toxicol Appl Pharmacol 239:87–97.

Kischkel FC, Lawrence DA, Tinel A, LeBlanc H, Virmani A, Schow P, Gazdar A, Blenis J, Arnott D, Ashkenazi A. 2001. Death receptor recruitment of endogenous caspase-10 and apoptosis initiation in the absence of caspase-8. J Biol Chem 276:46639–46646.

Kuo PL, Lin TC, Lin CC. 2002. The antiproliferative activity of aloe-emodin is through p53-dependent and p21-dependent apoptotic pathway in human hepatoma cell lines. Life Sci 71:1879–1892.

Lau AT, Wang Y, Chiu JF. 2008. Reactive oxygen species: Current knowledge and applications in cancer research and therapeutic. J Cell Biochem 104:657–667.

Lee HZ, Lin CJ, Yang WH, Leung WC, Chang SP. 2006. Aloe-emodin induced DNA damage through generation of reactive oxygen species in human lung carcinoma cells. Cancer Lett 239:55–63.

Lin ML, Lu YC, Chung JG, Li YC, Wang SG, N GS, Wu CY, Su HL, Chen SS. 2010. Aloe-emodin induces apoptosis of human nasopharyngeal carcinoma cells via caspase-8-mediated activation of the mitochondrial death pathway. Cancer Lett 291:46–58.

Lu GD, Shen HM, Chung MC, Ong CN. 2007. Critical role of oxidative stress and sustained JNK activation in aloe-emodin-mediated apoptotic cell death in human hepatoma cells. Carcinogenesis 28:1937–1945.

Martin DA, Siegel RM, Zheng L, Lenardo MJ. 1998. Membrane oligomerization and cleavage activates the caspase-8 (FLICE/MACHalpha1) death signal. J Biol Chem 273:4345–4349.

McDonald ER III, El-Deiry WS. 2004. Suppression of caspase-8- and -10-associated RING proteins results in sensitization to death ligands and inhibition of tumor cell growth. Proc Natl Acad Sci USA 101:6170–6175.

Mijatovic S, Maksimovic-Ivanic D, Radovic J, Miljkovic D, Harhaji L, Vuckovic O, Stosic-Grujicic S, Mostarica Stojkovic M, Trajkovic V. 2005. Anti-glioma action of aloe emodin: The role of ERK inhibition. Cell Mol Life Sci 62:589–598.

Mueller SO, Stopper H. 1999. Characterization of the genotoxicity of anthraquinones in mammalian cells. Biochim Biophys Acta 1428:406–414.

Nylander K, Dabelsteen E, Hall PA. 2000. The p53 molecule and its prognostic role in squamous cell carcinomas of the head and neck. J Oral Pathol Med 29:413–425.

Ott M, Norberg E, Zhivotovsky B, Orrenius S. 2009. Mitochondrial targeting of tBid/Bax: A role for the TOM complex? Cell Death Differ 16:1075–1082.

Ozoren N, Fisher MJ, Kim K, Liu CX, Genin A, Shifman Y, Dicker DT, Spinner NB, Lisitsyn NA, El-Deiry WS. 2000. Homozygous deletion of the death receptor DR4 gene in a nasopharyngeal cancer cell line is associated with TRAIL resistance. Int J Oncol 16:917–925.

Pan MH, Chiou YS, Chen WJ, Wang JM, Badmaev V, Ho CT. 2009. Pterostilbene inhibited tumor invasion via suppressing multiple signal transduction pathways in human hepatocellular carcinoma cells. Carcinogenesis 30:1234–1242.

Penninger JM, Kroemer G. 2003. Mitochondria, AIF and caspases—Rivaling for cell death execution. Nat Cell Biol 5:97–99.

Rousseau D, Cannella D, Boulaire J, Fitzgerald P, Fotedar A, Fotedar R. 1999. Growth inhibition by CDK-cyclin and PCNA binding domains of p21 occurs by distinct mechanisms and is regulated by ubiquitin-proteasome pathway. Oncogene 18:3290–3302.

Sedlak TW, Oltvai ZN, Yang E, Wang K, Boise LH, Thompson CB, Korsmeyer SJ. 1995. Multiple Bcl-2 family members demonstrate selective dimerizations with Bax. Proc Natl Acad Sci USA 92:7834–7838.

Song JD, Kim KM, Kim KH, Kim CD, Kim JM, Yoo YH, Park YC. 2008. Differential role of diphenyleneiodonium, a flavoenzyme inhibitor, on p53-dependent and -independent cell cycle progression. Int J Oncol 33:1299–1306.

Tsujimoto Y. 2003. Cell death regulation by the Bcl-2 protein family in the mitochondria. J Cell Physiol 195:158–167.

Vincenz C, Dixit VM. 1997. Fas-associated death domain protein interleukin-1beta-converting enzyme 2 (FLICE2), an ICE/Ced-3 homologue, is proximally involved in CD95- and p55-mediated death signaling. J Biol Chem 272:6578–6583.

Viswanath V, Wu Y, Boonplueang R, Chen S, Stevenson FF, Yantiri F, Yang L, Beal MF, Andersen JK. 2001. Caspase-9 activation results in downstream caspase-8 activation and bid cleavage in 1-methyl- 4-phenyl-1,2,3,6-tetrahydropyridine- induced Parkinson's disease. J Neurosci 21: 9519–9528.

Wang D, Yu X, Brecher P. 1998. Nitric oxide and N-acetylcysteine inhibit the activation of mitogen-activated protein kinases by angiotensin II in rat cardiac fibroblasts. J Biol Chem 273:33027–33034.

Wang J, Chun HJ, Wong W, Spencer DM, Lenardo MJ. 2001. Caspase-10 is an initiator caspase in death receptor signaling. Proc Natl Acad Sci USA 98: 13884–13888.

Xia Z, Dickens M, Raingeaud J, Davis RJ, Greenberg ME. 1995. Opposing effects of ERK and JNK-p38 MAP kinases on apoptosis. Science 270:1326–1331.

Xu SQ, El-Deiry WS. 2000. p21(WAF1/CIP1) inhibits initiator caspase cleavage by TRAIL death receptor DR4. Biochem Biophys Res Commun 269:179–190.

Zhu H, Zhang L, Wu S, Teraishi F, Davis JJ, Jacob D, Fang B. 2004. Induction of S-phase arrest and p21 overexpression by a small molecule 2[[3-(2,3-dichlorophenoxy)propyl] amino]ethanol in correlation with activation of ERK. Oncogene 23:4984–4992.